Int. J. Electrochem. Sci., 13 **(2018)** 1293 – 1307, doi: 10.20964/2018.02.04

International Journal of
ELECTROCHEMICAL
SCIENCE
www.electrochemsci.org

Gold Nanoparticle-Decorated Single-Walled Carbon Nanotubes as a Catalytic Amplification Platform for the Electrochemical Detection of Alkaline Phosphatase Activity

Lingzhi Zhao[1,2,*], *Liu Zhao*[3], *Yanqing Miao*[1], *Chenxiao Zhang*[2,*]

[1] College of pharmacy, Xi 'an Medical College, Xi 'an 710021, China
[2] Key Laboratory of Analytical Chemistry for Life Science of Shaanxi Province, School of Chemistry and Chemical Engineering, Shaanxi Normal University, Xi'an 710062, China
[3] Beijing Research Center of Agricultural Standards and Testing, Beijing 100097, China
[*]E-mail: oldskyhappy_zlz@163.com

Received: 8 October 2017 / *Accepted:* 29 November 2017 / *Published:* 28 December 2017

The detection of alkaline phosphatase (ALP) activity is of great significance in many biomedical applications and for understanding the functional mechanism of ALP-related biological events. A sensitive electrochemical ALP biosensor using ascorbic acid 2-phosphate (AA-P) as the substrate was developed based on a gold nanoparticle-decorated single-walled carbon nanotube (GNP/SWNT)-modified glassy carbon electrode (GCE). The activity of ALP was determined indirectly according to the concentration of ascorbate (AA), which was generated during the hydrolysis reaction of AA-P in the presence of ALP as a catalyst. The biosensor exhibited a low applied potential, high sensitivity and selectivity, and the current response increased with ALP concentration from 3 to 50 U L^{-1} with a detection limit of 0.2 U L^{-1}. The applicability of the developed method was demonstrated for successfully detecting ALP in whole HeLa cell lysate, thus providing a promising tool for other sensing systems that involve ALP.

Keywords: Alkaline phosphatase activity, Gold particles, Single-walled carbon nanotubes (SWNTs), whole cell lysate.

1. INTRODUCTION

Alkaline phosphatase (ALP) (EC 3.1.3.1), one of the most common enzymes that exists in mammalian tissues, is a non-specific phosphomonoesterase that can catalyze the hydrolysis reaction of a wide variety of phosphoric acid monoesters in alkaline media including biological macromolecules (such as nucleic acids, proteins, and carbohydrates) and small organic molecules [1-2]. An abnormal

level of ALP activity has been associated with a number of diseases such as liver dysfunction [3], adynamic bone disease [4], breast and prostate cancers [5], and diabetes [6]. Thus, simple, sensitive and exact ALP detection methods are highly desired in clinical diagnoses and many biomedical applications.

The routine assessment of ALP activity utilizes ALP substrates for the detection of enzymatically generated products via various monitoring techniques and methods. The most frequently described detection methods are electrochemistry[7-10], electrochemiluminescence [11-12], colorimetric[13-15] and fluorescence assays [16-20,23-25]. Among these methods, owing to the low detection limit, fast response, versatile design and ease of miniaturization, growing interest has been focused on electrochemical methods based on the direct detection or electrocatalytic approach. The future development of electrochemical methods for ALP activity assays depends on the selection of suitable substrates that can be converted by the enzyme to an electrochemical active product. Additionally, the substrate should be chemically stable and electrochemically inactive at the detected potential, while the product should have good electrochemical activity with rapid electron transfer to the electrode and should be able to be detected at a relatively low potential. The common substrates in the electrochemical detection of ALP activity are phosphorylated phenols such as 1-naphthol phosphate, p-nitrophenyl phosphate, p-aminophenyl phosphate, etc. The oxidation peak potential of most phenols appears at approximately 0.200 V, suggesting that there are potential interferences from other electroactive species at this potential. To fulfill the requirements of high sensitivity and minimum interference, in this work, ascorbic acid 2-phosphate (AA-P) was chosen as the substrate for the electrochemical detection of ALP activity based on the different electrochemical responses of the enzyme substrate AA-P and product ascorbate (AA) on the as-prepared electrodes. The oxidation current of AA can determine indirectly ALP.

The previous work of our group has displayed the proposed mechanism for the electrooxidation of the ALP-catalyzed product AA [21]. AA can be electrochemically oxidized through a two electron and one-proton pathway, and SWNTs can facilitate the oxidation of AA at a low potential, approximately -0.100 V, which avoids interferences from other electroactive species at such a low potential. On this basis, the purpose of this work was to develop a highly sensitive and selective electrochemical method for the determination of ALP activity in biosamples such as cancer cell lysate. Herein, for the first time, an electrochemical biosensor for the ALP-catalyzed product AA was developed using dual signal amplification of SWNTs and gold nanoparticles (GNPs). The principle scheme is demonstrated in Scheme 1. The GNP /SWNT biocomposite denotes efficient electrocatalytic function and faster electron-transfer kinetics for the electrochemical oxidation behavior of AA at -0.100 V. Compared to the reported electrochemical methods with phosphorylated phenols as the enzyme substrate, the main advantage of the present method is its high selectivity for the detection of the ALP-catalyzed product AA. Such a low oxidation potential avoids interference from other bioactive substances coexisting with AA in biological samples. With this striking analytical performance, the developed method is applied for the sensitive detection of AA and selective determination of ALP activity in whole HeLa cell lysate, which could be potentially useful in physiological metabolic process research and in clinical diagnosis.

2. EXPERIMENTAL SECTION

2.1. Apparatus and reagents

Ascorbic acid 2-phosphate (AA-P), dopamine (DA), lactate, glucose, and sodium ascorbate (AA) were all purchased from Sigma-Aldrich. The amino acids were obtained from Aladdin company. Dulbecco's modified Eagle Medium (DMEM, high glucose) was obtained from Gibco Invitrogen, Carlsbad, CA. Fetal bovine serum (FBS, South American Origin) was obtained from HyClone. Single-walled carbon nanotubes (with an average diameter less than 2 nm, SWNTs), and reduced graphene oxide (rGO) and graphene oxide (GO) were obtained from Chengdu Organic Chemicals Co., Ltd., Chinese Academy of Sciences (Chengdu, China). A 0.1 M phosphate-buffered saline (PBS) solution was prepared containing 136.7 mM NaCl, 2.7 mM KCl, 0.087 M Na_2HPO_4, and 0.014 M KH_2PO_4, using NaOH and HCl to adjust the pH. Aqueous solutions of AA-P, and AA were freshly prepared with PBS. A mixture of amino acids in 0.1 M PBS at pH 9.0 was prepared containing tryptophan, cysteine, glutamic acid, tyrosine, arginine, homocysteine, lysine, and phenylalanine (the final concentrations for every kind of amino acid was 50 μM), a mixture of metal ions in 0.1 M PBS at pH 9.0 was prepared containing Fe^{3+}, Fe^{2+}, Zn^{2+}, Al^{3+}, Pb^{2+}, and Cu^{2+} (the final concentrations for every type of metal ion was 20 μM), All reagents were at least analytical grade and used as received. Aqueous solutions were prepared with Milli-Q water.

Cyclic voltammetry (CV) was performed on an electrochemical analyzer (CHI 660E, CH Instruments) with a GCE as the working electrode, a Pt wire as the counter electrode and a Ag/AgCl electrode (KCl-saturated) as the reference electrode. All potentials were referred to with respect to this reference electrode. Transmission electron microscopy (TEM) studies were carried out with the Tecnai G2 F20 microscope (FEI Company, USA) operating at a 200 kV accelerated voltage.

2.2. Enzymatic assay for ALP

The GC electrodes (2.0 mm diameter) and Au electrodes (1.6 mm in diameter) were successively polished with 0.3 and 0.05 μm alumina slurries on a polishing cloth, cleaned under bath sonication for 5 min in acetone and distilled water, and thoroughly rinsed with Milli-Q water. The Au electrode was then electrochemically pretreated by consecutively cycling the potential between -0.2 and +1.6 V at 0.5 V s^{-1} in a 0.5 M H_2SO_4 solution until a cyclic voltammogram characteristic of a clean Au electrode was obtained. One milligram SWNTs were dispersed into 1 mL N,N-dimethylformamide (DMF) to obtain a homogeneous suspension under sonication, followed by drop-coating 3 μL of the prepared suspension onto the surface of cleaned GC electrodes to obtain the SWNT-modified electrodes (SWNT/GCEs). The procedures for the electrodeposition of gold nanoparticles (GNPs) on SWNT/GCEs agreed with reference [22]: GNPs were electrodeposited on the electrode by maintaining a constant potential of + 1.1 V (vs. Ag/AgCl, sat. KCl) for 60 s and then a constant potential of -0.1 V for 10 min at the desired electrode in 0.1 M $HClO_4$ containing 0.1% $HAuCl_4$. For the graphite-modified GCE, a 2 mg/mL portion of graphite powder was dispersed into N,N-dimethylformamide

followed by drop-coating 2 μL of the dispersion onto the GC electrode. The electrode was then air-dried to evaporate the solvent to obtain the graphite-modified GCE.

Electrochemical measurements of the ALP-catalyzed substrate and products (AA-P, AA) were performed on the modified GCE and Au electrode in 0.1 M PBS. For ALP activity in the solution, AA-P in PBS was preincubated with different concentrations of ALP for 15 min. The current signals were then recorded. The CV measurements were performed at a rate of 0.05 V s^{-1} in the potential range from -0.4 to 0.6 V. For ALP activity on the electrode, 2 μL of the aqueous solution of ALP (50 U L^{-1}) was mixed with 1 μL of the aqueous solution of BSA (1 wt.%) and 1.5 μL of the aqueous solution of glutaraldehyde (1 wt.%), and the as-obtained mixture was dropped onto a clean GNP/SWNT-modified GCE.

2.3 Cell culture and electrochemical determination of alkaline phosphatase activity in whole HeLa cell lysate

Human cervical carcinoma cells (HeLa cells, Xi'an Medical University) were cultured in a DMEM medium supplemented with 10% fetal bovine serum, penicillin (100 μg/mL), and streptomycin (100 μg/mL) in a humid incubator (5% CO_2, 37°C). The cell number was determined using a traditional counting chamber (Thoma). A Leica inverted microscope (DMI 6000) equipped with a digital monochrome camera (Leica DFC 350 FX) with software provided by Leica (LAS AF) was used to visualize the cells. The lysis buffer for the HeLa cells was prepared and contained 50 mM Tris–HCl, 150 mM NaCl, and 0.1% Triton x-100, and the pH was adjusted to 9.0.

For the alkaline phosphatase extractions, first, the cells were washed twice with 0.1 M PBS (pH 7.4). All subsequent procedures were carried out at +4°C. The cells were scraped and collected into the 0.5 mL lysis buffer, then homogenized in a vortex mixer for 20 min. The homogenate was centrifuged at 20000 × g for 10 min. The supernatant was collected into a fresh tube as the alkaline phosphatase extraction. For the electrochemical detection of alkaline phosphatase activity in whole HeLa cell lysate, the substrate AA-P was directly dispersed in the alkaline phosphatase extraction, the final concentration is 3 mM, and the mixture was incubated at 37°C for 10 min for subsequent detection.

3. RESULTS AND DISCUSSION

3.1. Cyclic voltammetric response of the enzyme substrate and product (AA-P, AA) at different modified GCEs

Simple, sensitive and selective detection methods for bio-related molecules and enzymes exhibit extremely important roles in metabolic process research and clinical diagnosis. In the previous work of our group, a comparison of the voltammograms obtained for ascorbate (AA) oxidation at various electrodes clearly demonstrates that AA oxidation at SWNT- and heat-treated SWNT-modified electrodes located at a more negative potential exhibits a faster electron-transfer kinetics than GC and graphite-modified GC electrodes, suggesting the efficient electrocatalytic function of SWNTs [21].

Based on these results, in this work, the ALP activity assays with high sensitivity and selectivity will be developed. As displayed in Scheme 1, the oxidation current of AA on the as-prepared electrode was applied to determine indirectly the ALP activity. The method is based on the fact that ALP as the catalyst can catalyze the hydrolysis of AA-P and trigger the release of AA. The latter can produce electrochemical signals at the electrode surfaces, while the AA-P substrate exhibit no electrochemical signals. Based on the various electrochemical responses of the enzyme substrate and product on the as-prepared electrodes, the ALP activity can be sensitively determined.

Figure 1A and 1B compare the oxidation of 3 mM AA at different kinds of modified electrodes. As shown, at the bare GCE (d), graphite-modified GCE (c), GO-modified GCE (b) and Au electrode (e), the oxidation of AA occurs irreversibly at +0.20 V, +0.19 V, +0.29 V and +0.30 V, respectively. The oxidation current value for the abovementioned electrodes did not exceed 20 μA. At the rGO-modified electrode, the oxidation of AA occurs at -20 mV with a response of less 20 μA. At the SWNT-modified GCE (g) and GNPs /SWNT-modified GCE (f), the oxidation of AA occurs at -70 mV with oxidation current values of approximately 150 and 180 μA, respectively. These observations manifest the efficient electrocatalytic function of the SWNT/GCE or GNPs /SWNT-modified GCE and the faster electron-transfer kinetics towards the electrochemical oxidation behavior of AA. In view of the higher peak current for AA oxidation at the GNP /SWNT-modified GCE, the GNP/SWNT nanocomposites were chosen as the modified material for the subsequent ALP activity assays in this work.

To further examine the feasibility of the as-designed sensing method, we studied the electrochemical behavior of the substrate AA-P at the corresponding electrodes. As shown in Figure 1C and 1D, no corresponding oxidation or reduction peak appeared for 3 mM AA-P. These results clearly demonstrated that the electrochemical detection of ALP activity using AA-P as the substrate is feasible. It should be noted that a pair of redox waves was observed at a potential of 0.0 V (Fig. 1C), which were not generated from AA-P electrochemical behavior but were from the characteristic redox process of oxygen-containing moieties produced at the SWNTs, which had been verified in the previous work of our group[21].

Under physiological conditions, with PBS at pH 7.4, the analytical performance of GNP /SWNT-modified GCE was investigated by cyclic voltammetry with different concentrations of AA. As shown in Figure 2, a well-defined increase in the oxidation peak current at approximately -0. 70 V was observed with successive increments of AA in the AA concentration range from 0.3 mM to 5 mM, the linear equation was I (μA) = 52.05 C_{AA} (μM) – 9.886 (R =0.986), and the detection limit of AA was 0.01 mM. The assay displayed good performance in the detection limit and the linear range, which was attributed to the excellent catalytic properties of the GNP /SWNT nanocomposites. Since the method is based on the oxidation current of AA on the GNP /SWNT/GCE to indirectly determine ALP activity, these results evidently manifested that the use of GNP /SWNT nanocomposites and AA-P as the substrate for the ALP activity assays are successful.

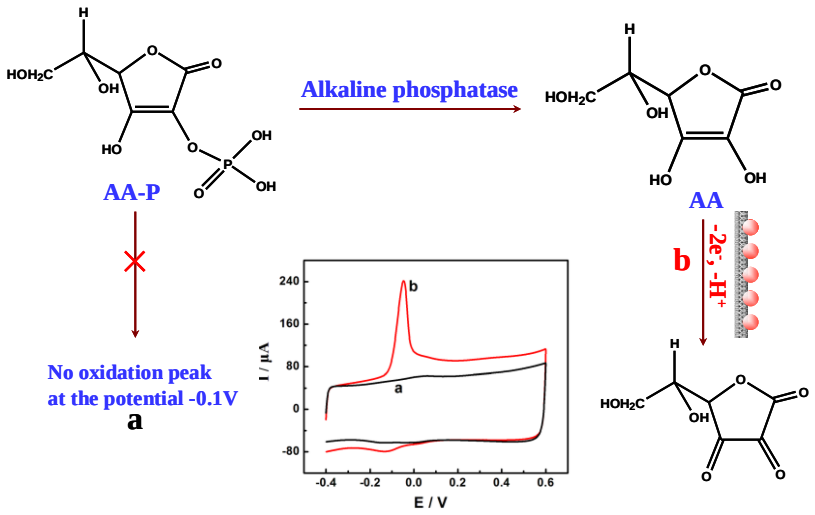

Scheme 1. The proposed mechanism for detecting ALP activity by using the GNP/SWNT nanocomposite.

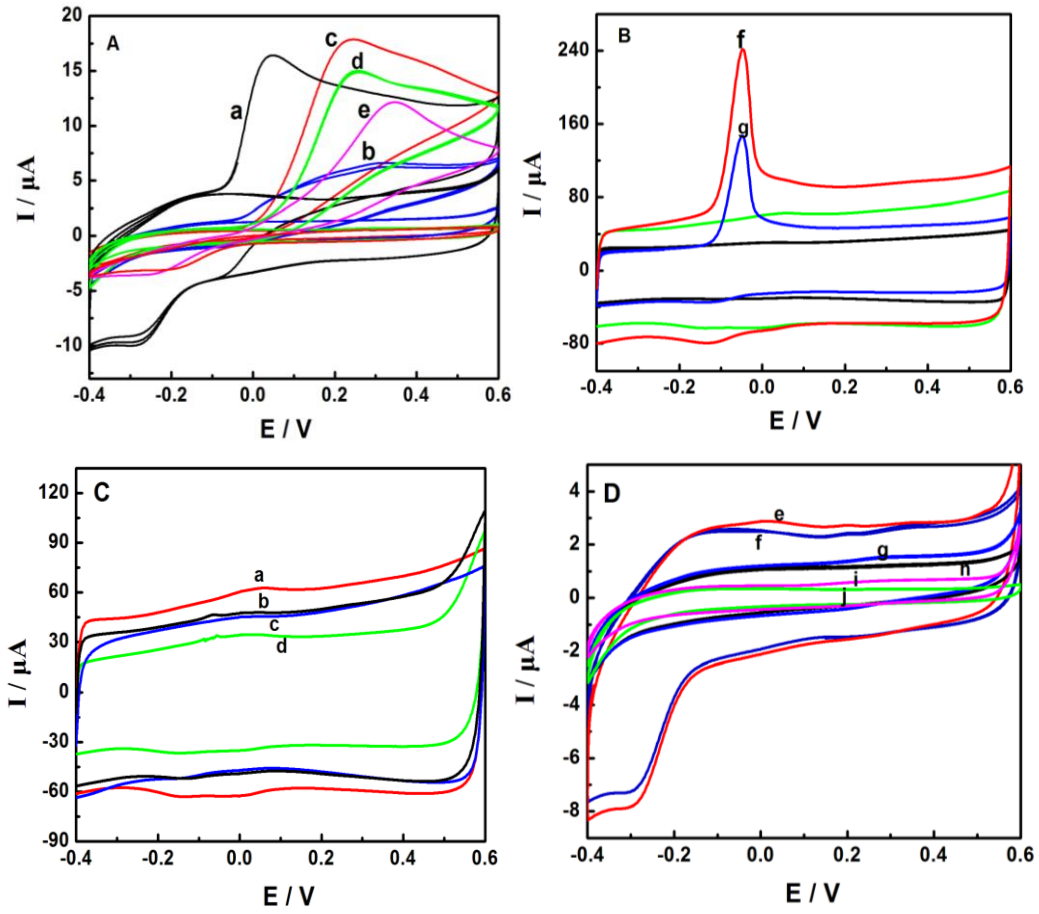

Figure 1. (A) and (B). Typical cyclic voltammograms (CVs) obtained at the bare GC (d), rGO-modified (a), GO-modified (b), graphite-modified (c), SWNT-modified (g), and GNP /SWNT-modified (f) GC electrodes and Au electrode (e) in 0.10 M PBS (pH 7.4) in the absence and presence of 3 mM AA. (C) and (D). Typical cyclic voltammograms (CVs) obtained at the bare GC (g), rGO-modified (e), SWNT-modified (b), GNP/SWNT-modified (a) GC electrodes and Au electrode (i) in 0.10 M PBS (pH 7.4) in the absence and presence of 3 mM AA-P. Scan rate, 50 mV s^{-1}.

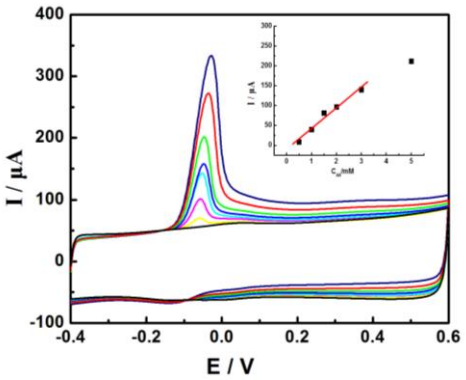

Figure 2. CVs and plot of Ip (μA) versus C_{AA} at the GNP /SWNT-modified GCE in different concentrations of AA (from bottom to top: 0, 0.5, 1, 1.5, 2, 3, 5, and 10 mM) in 0.10 M PBS (pH 7.4). Scan rate, 50 mV s^{-1}.

3.2. Characterization of the GNP /SWNT *nanocomposites*

Transmission electron microscopy (TEM) was used to characterize the morphologies of the as-prepared GNP/SWNT nanocomposites and directly monitor the formation of GNPs on the SWNTs. These TEM profiles demonstrate an obvious difference in the SWNT morphology between the pristine SWNTs and GNPs /SWNTs. In detail, it is observed that large amounts of microcubes with sizes of several micrometers and quite smooth surfaces were observed from the net SWNTs in Figure 3A. In contrast, as shown in Figure 3B, the surface of the SWNTs was modified with homogeneous spherical nanoparticles, indicating that there was a substantive formation of GNPs on SWNTs by using the electrodepositing method. Herein, there are two functions of GNPs in this work. One is the amplification of the active surface area, and the other is providing more biocompatible sites for the cross-linking of ALP, as demonstrated later.

Moreover, the different interfaces of the modified electrodes were evaluated by monitoring the change in the electron-transfer resistance (R_{et}) using electrochemical impedance spectroscopy (EIS) and conductivity using cyclic voltammetry with $[Fe(CN)_6]^{3-/4-}$ as the redox probe (Fig. 3C and Fig. 3D). As shown in Fig. 2C, EIS included a semicircular portion at higher frequencies and a linear portion at lower frequencies, which corresponds to R_{et} and the diffusion process, respectively. R_{et} (Fig. 3C, c) at the GNP /SWNT-modified GCE was much smaller than that at a bare GCE (Fig. 3C, a) or was slightly smaller than the SWNT-modified GCE (Fig. 3C, b), suggesting that both GNPs and SWNTs can both accelerate the electron transfer of $[Fe(CN)_6]^{3-/4-}$ due to their excellent electronic conductivity. To attain better electrochemical responses, GNPs and SWNTs were combined as the nanocomposite for dual signal amplification. The CV data also showed perfectly good agreement with the above results of the Nyquist plots (Fig. 3D). The results demonstrate again that GNPs have successfully been synthesized on the SWNT-modified GCE by using an electrodeposition method to catalyze the electrochemical oxidation of AA at a low potential.

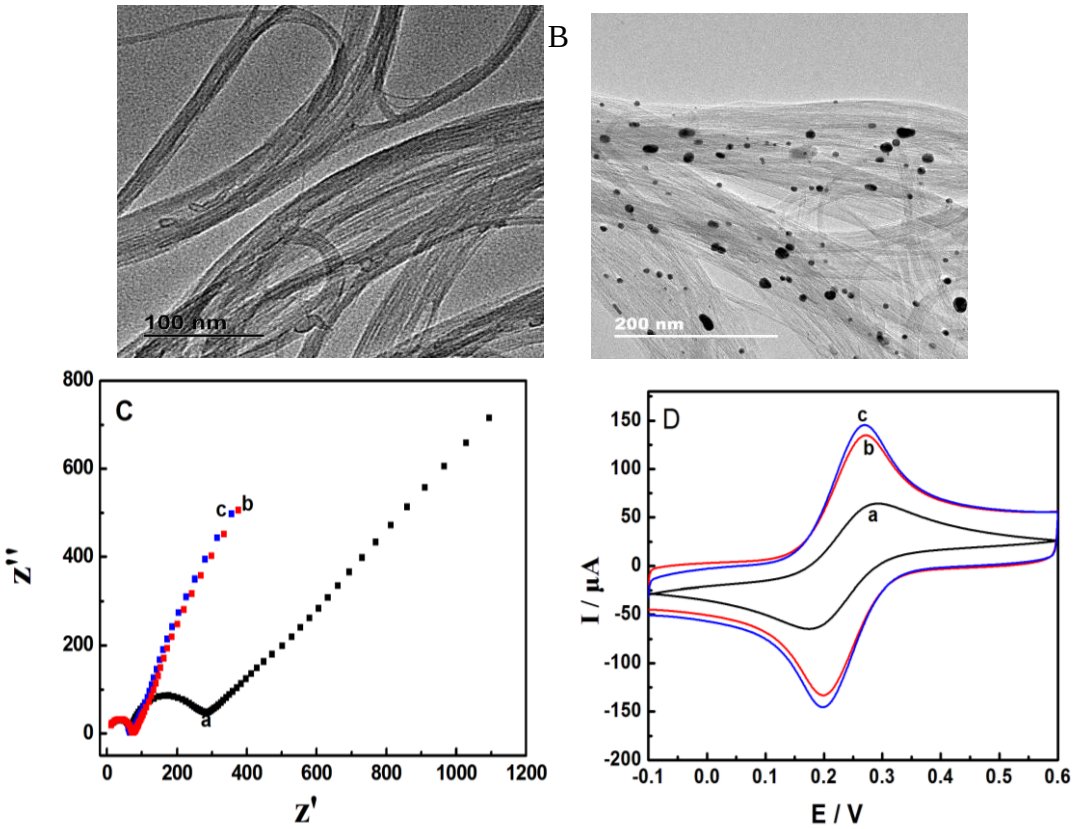

Figure 3. TEM images of (A) SWNTs and (B) GNP-electrodeposited SWNTs. Nyquist plots of the impedance spectra (C) and cyclic voltammograms (D) of different electrodes in 0.1 M PBS (pH 7.4) containing 5 mM $[Fe(CN)_6]^{3-}$/$[Fe(CN)_6]^{4-}$: a) bare GC, b) SWNT-modified, and c) GNP /SWNT-modified GCE. The biased potential was + 0.25 V. The frequency was from 1 Hz to 100 kHz, and the amplitude was 5.0 mV. Scan rate, 100 mV/s.

3.3 Effect of pH

Since the electrochemical behaviors of the ALP-hydrolyzed product AA and ALP activity both depend on the pH value of the detection solution, to attain a high sensitivity, the effect of pH on the electrochemical behaviors was studied at the GNP /SWNT/GCE with typical pH values (pH 4.5, pH 7.4, pH 9.0) in the presence of 3 mM AA. The pH value of 7.4 was chosen because the pH value of the physiological condition is 7.4, whereas pH 9.0 was chosen because ALP exhibits maximum activity at pH 9.0. As shown in Fig. 4, the oxidation peak currents increased with an increase in pH, and the largest current response appeared at pH 9.0, indicating that an alkaline condition was beneficial to the electrochemical processes for AA oxidation. In addition, the redox peak potentials negatively shift gradually with an increase in pH value, suggesting that H^+ participated in this process. The previous work of our group has displayed the proposed mechanism for the electrooxidation of AA [21]. AA is a water-soluble hexonic sugar acid and has two dissociable protons with pKa values of 4.2 and 11.8, which means that AA is a monovalent anion at pH 7.4 or pH 9.0. Further, AA should be electrochemically oxidized through a two-electron and one-proton pathway (Scheme 1), which can explain the phenomenon of a negative shift in the potential. Since the higher peak current response for AA oxidation was obtained in an alkaline condition pH 9.0 and ALP also exhibits maximum activity at

pH 9.0, 0.1 M PBS (pH 9.0) was selected as the pH buffer for the subsequent ALP activity assays in this work.

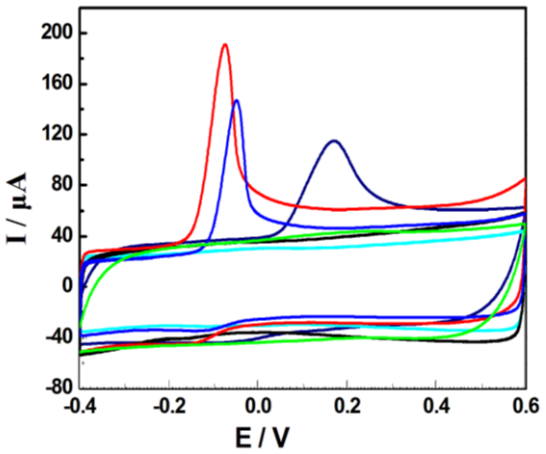

Figure 4. CVs obtained in different pH buffer solutions containing 3 mM AA with GNP /SWNT-modified GC electrodes. From left to right: 0.10 M PBS (pH 9.0, pH 7.4, pH 4.5).

3.4. Assay performance for the detection of ALP activity based on GNP /SWNT nanocomposites

Alkaline phosphatase (ALP) is one of the most important hydrolase that exists in different tissues. ALP assays generally utilize ALP substrates and detect enzymatically generated products to indirectly reflect the ALP activity. Herein, AA-P was chosen as the substrate for the electrochemical detection of ALP activity, and the oxidation current of AA can determine indirectly the ALP activity. By empirically optimizing the detection conditions, the following optimal parameters were identified: a 60-s electrodeposition time for the GNPs and a 15-min incubation time. For the ALP activity in the solution, 3 mM AA-P in PBS (pH 9.0) was incubated with varying units of ALP for 15 min, the oxidation current signals at the GNP /SWNT-modified GCE were then recorded. Figure 5 displayed typical voltammetric responses toward 3 mM AA-P incubated with different concentrations of ALP, and the results indicate that almost no current response was observed from the AA-P solution without the presence of ALP. In contrast, a well-defined increase in the oxidation peak current at approximately -0.100 V was observed with an increase in ALP activity, Fig. 5 inset shows the calibration curve for the ALP assay, and the linear equation was I (μA) = 3.4947 C_{ALP} (U L^{-1}) + 1.7737 (R =0.982) in the range from 3 U L^{-1} to 10 U L^{-1}. The detection limit of the ALP concentration based on a signal-to-noise ratio of 3 (S/N = 3) was calculated to be 0.2 U L^{-1}. Compared with other methods for the ALP activity assay, the as-established electrochemical method displayed good performance regarding the detection limit and linear range. For example, our system was comparable and even more efficient for the detection of ALP activity compared to existing methods (Table 1). More importantly, the obvious advantage of this study is the simplicity and effectiveness in using AA-P as the substrate, in which the hydrolysis product had a lower oxidation potential, demonstrating the high selectivity compared with other species, as described later.

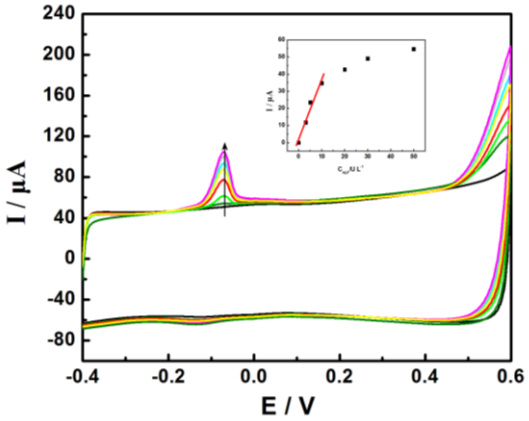

Figure 5. CVs and plots of Ip (μA) versus C_{ALP} in the presence of 3 mM AA-P with different concentrations of ALP from bottom to top (0, 3, 5, 10, 20, 30 and 50 U L^{-1}) at the GNPs /SWNTs-modified GC electrode in 0.1 M PBS at pH 9.0. Scan rate, 50 mV s^{-1}.

Table 1. Analytical performance for the ALP activity assay.

Detection technique	Materials used	Detection limit	Linear range	Sample analysis	Reference
Differential pulse voltammetry	Copper sulfide nanoparticle-decorated graphene	0.02 U L^{-1}	0.1 to 100.0 U L^{-1}	serum samples	7
Cyclic voltammetry	Sodium molybdate-decorated graphene oxide	0.5 U L^{-1}	1.0 to 500.0 U L^{-1}	No	10
Differential pulse voltammetry	Single molecular beacon-initiated T7 exonuclease mediated signal amplification	0.1 U L^{-1}	0.1 to 10.0 U L^{-1}	No	8
Fluorescent strategy	Resazurin	0.12 U L^{-1}	0.6 to 6.0 U L^{-1}	diluted serum samples (0.2% fetal bovine serum).	23
Fluorescent strategy	Infinite coordination polymer (ICP) nanoparticles: the coumarin@Tb-GMP suspension	0.010 U mL^{-1}	0.025 U mL^{-1} to 0.2 U mL^{-1}	No	20
Fluorescent strategy	polyethyleneimine-capped copper nanoclusters and the MnO_2 nanosheets	0.27 U L^{-1}	0.5 to 200.0 U L^{-1}	dilute human serum (5%)	24
Fluorescent strategy	graphene quantum dots and para-benzoquinone (BQ).	0.45 U L^{-1}	1.0 to 90.0 U L^{-1}	dilute serum samples	25
Colorimetric and SERS dual-readout	Ag-coated Au nanoparticles	0.10 U L^{-1}	0.5 to 10.0 U L^{-1}	No	15
Electrochemilumi nescence	CdSe nanoparticles	2.0 U L^{-1}	2.0 to 25.0 U L^{-1}	diluted serum samples	11
Cyclic voltammetry	Gold nanoparticle-decorated single-walled carbon nanotubes	0.2 U L^{-1}	3.0 to 50.0 U L^{-1}	whole HeLa cell lysate	This work

3.5 Detection of AA-P at the ALP/GNP/SWNT-modified GCE biosensor

ALP was dropped onto the ALP GNP /SWNT-modified GC electrodes to develop a biosensor based on the immobilization of ALP on the electrode. Considering that the enzymatic activity is inhibited by the presence of heavy metals, insecticides, nerve gases, etc., enzyme-based biosensors are important tools to detect these toxic chemicals for healthcare applications, the food industry, environmental analyses, etc. [26-27]. The ALP biosensor was explored by CV measurements at an applied potential of 0.0 V vs. Ag/AgCl. The resulting ALP/GNP/SWNT-modified GCE exhibits good bioelectrocatalytic activity for the oxidation of AA that originated from ALP-catalyzed AA-P hydrolysis, which commences at -0.1 V, as shown in Figure 6A. After the immobilization of ALP onto the GNP/SWNT-modified GCE, a well-defined current response was recorded for AA-P at the ALP/GNP/SWNT-modified GC electrode and the current responses reached their maximum values in a short time, suggesting good sensing properties of the ALP-based biosensors with GNPs and SWNTs as the electrocatalysts for the oxidation of the ALP–hydrolyzed product AA.

Figure 6B shows the amperometric response at the ALP/GNP/SWNT-modified GCE at 0.0 V in a stirred solution on the successive addition of AA-P. With increasing AA-P concentration, the amperometric response of the biosensor increased in the range from 0.1 to 3 mM. The response current increased with increasing AA-P concentration, and the calibration curve was I (μA) = 2.3407 C_{AA-P} (mM) + 0.3369 (R =0.987) in the range from 0.1 mM to 1.5 mM. Additionally, the detection limit of ALP concentration based on a signal-to-noise ratio of 3 (S/N = 3) was calculated to be 20 μM. The higher AA-P concentrations have the lower amperometric responses; furthermore, when the concentration of AA-P exceeded 3 mM, the amperometric response gradually leaned toward a constant value, indicating that the ALP catalytic reaction changed from the first to zero order, which agrees with the characteristic of Michaelis–Menten kinetics. The experiments showed that the resulting AA-P biosensors based on the ALP/GNP/SWNT biocomposite exhibited a rapid and sensitive response to the change in AA-P concentration, which could be potentially useful for evaluating the enzyme inhibitor efficiency and may be further applied to monitor toxic chemicals in the environment.

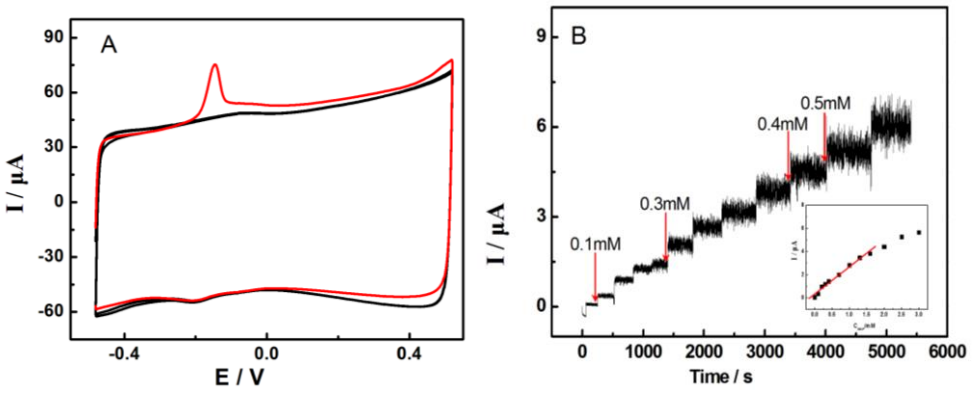

Figure 6. (A) CVs at the ALP/GNP /SWNT-modified GC electrodes in the absence and presence of 3.0 mM AA-P in 0.1 M PBS at pH 9.0. Scan rate, 50 mV s^{-1} (B) Typical current–time plot for the sensor with the successive addition of stock AA-P to 0.1 M PBS (pH 9.0) at 0.00 V vs. Ag/AgCl. The insert shows the linear relationship between the peak current values and the concentration of AA-P.

3.6 Interference study

The selectivity of the GNP/SWNT-modified GCE towards AA-P activity was assessed by testing the specific enzyme (5 U L^{-1} ALP) and nonspecific enzymes (other proteins and enzymes, including BSA, GOx, lysozyme, and AChE) in the solution. A distinct increase in current (ΔCurrent = 16.2 μA) was observed for 5 U L^{-1} ALP, whereas a very slight increase in current was found for the other proteins and enzymes (Figure 7A). A distinct increase in ALP was ascribed to AA that is generated in the hydrolytic reaction and increased depending on the ALP activity under the condition of excess AA-P at the GNP /SWNT-modified GCE. These results indicate that the proposed strategy exhibited good selectivity for the ALP activity assays in the biosystem samples.

Moreover, the selectivity of the ALP/GNP/SWNT-modified GCE was evaluated by comparing its current response towards AA-P with the most common bioactive species, including glucose (0.5 mM), 6 types of metal ion mixtures, amino acids, citric acid, oxalic acid under the same detection conditions. The results demonstrated that no noticeable changes in the current signals were detected for the interfering species at the present operating potential in this system, suggesting that the proposed strategy based on ALP/GNPs/SWNTs biocomposite has a high selectivity towards the substrate AA-P, allowing potential applications in complex samples for screening enzyme inhibitors and determining toxic chemicals.

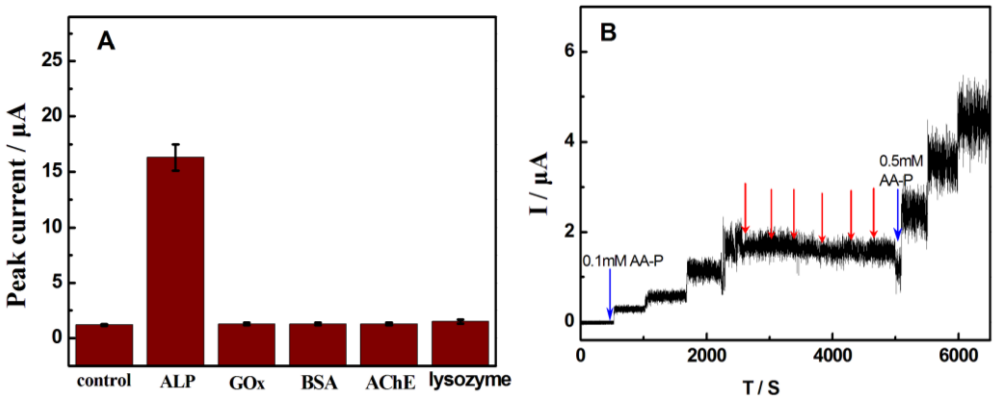

Figure 7. (A) A selectivity evaluation of the ALP activity assay at the GNP /SWNT-modified GCE was performed in 3 mM AA-P in 0.10 M PBS (pH 9.0) with blank, 5 U L^{-1} ALP or 20 U L^{-1} interferences including glucose oxidase (GOx), lysozyme, acetylcholinesterase (AChE) and 0.1 mg/mL bovine serum albumin (BSA). (B) Current-time responses obtained with the system towards species including glucose (0.5 mM), 6 types of metal ion mixtures (Fe^{3+}, Fe^{2+}, Zn^{2+}, Al^{3+}, Pb^{2+}, and Cu^{2+}, 50 μM), 3 types of anion mixtures (SO_4^{2-}, NO_3^-, and Cl^-, 100 μM), amino acid mixtures, citric acid (100 μM), and oxalic acid (50 μM), which were added in order. The other conditions were the same as those in Figure 6B.

3.7. Detection of ALP activity in whole HeLa cell lysate

To evaluate the applicability of the as-established detection method for the electrochemical detection of ALP activity in real samples, the ALP activity in whole HeLa cell lysate was detected as depicted in Figure 8. The black line displays the current response in the absence of the AA-P substrate.

For comparison, after the addition of AA-P into the whole HeLa cell lysate, it was observed that an oxidation peak appeared at -0.100 V, which was estimated as the peak current ascribed to the current response of AA. This finding indicates that ALP activity in the HeLa cell lysate was 0.8012 U L^{-1} for 5×10^5 cells•mL^{-1} and 1.8912 U L^{-1} for 1×10^6 cells•mL^{-1}, suggesting the existence of ALP in the HeLa cells. The applicability of the developed method was demonstrated for ALP activity in whole HeLa cell lysate, which could be potentially useful to measure ALP in clinical samples.

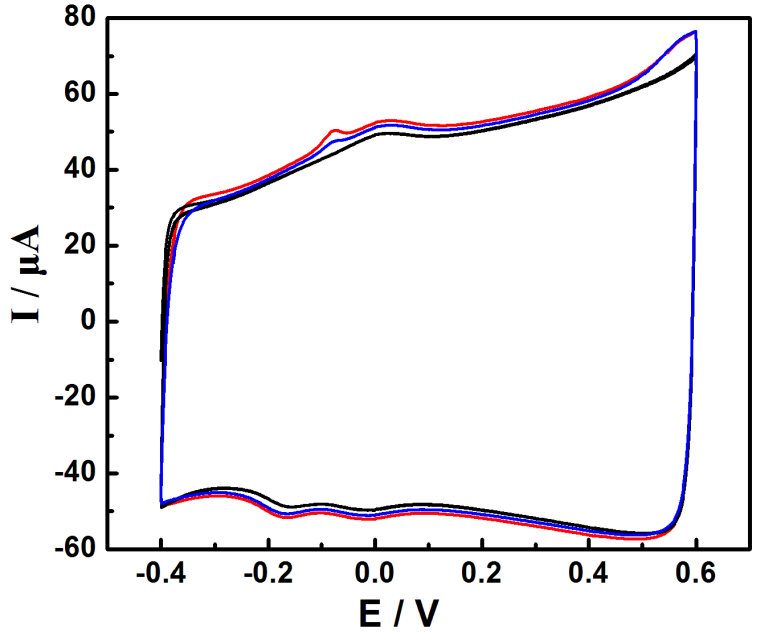

Figure 8. Typical CVs of 3 mM AAP obtained in 0.1 M PBS (pH 9) in the absence and presence of whole HeLa cells lysates. (Hela cells, 5×10^5 cells•mL^{-1}, 1×10^6 cells•mL^{-1}) at the GNP /SWNT-modified GC electrode. Scan rate, 50 mV s^{-1}.

4. CONCLUSIONS

This work is the first demonstration of the electrochemical detection of alkaline phosphatase (ALP) activity using ascorbic acid 2-phosphate (AA-P) as the substrate. The oxidation current of the ALP-catalyzed product ascorbate (AA) can indirectly determine ALP activity. By combining the virtues of carbon nanotubes and gold nanoparticles for efficient electrocatalytic activity towards AA oxidation, an electrochemical protocol was successfully developed for the selective detection of ALP activity. Compared with existing methods using phosphorylated phenols as the enzyme substrate, the main advantage of the present method is its high selectivity for detecting AA. AA is a good alternative for phenols and allows the sensitive and selective electrochemical detection at -0.10 V. Such a low oxidation potential avoids interference from other bioactive substances. The applicability of the developed method was demonstrated for the successful determination of ALP activity in the whole HeLa cell lysate, suggesting that the as-established method could be potentially useful in physiological metabolic process research and in clinical diagnosis.

ACKNOWLEDGEMENTS
This work is financially supported by NSF of China (Grant Nos. 21305109 for L. Zhao, 81701014 for D. Wang, and 91332101 for C. Zhang), by Open Fund Project Foundation of Institute of Medicine, Xi'an Medical University of China (No. 2016YXXK15) and by the Scientific Research Plan Projects Foundation of Shaanxi Science and Technology Department of China (No. 2014JQ2073, 2014K02-11-01)

References

1. J. E. Coleman, *Annual Review of Biophysics & Biomolecular Structure*, 21 (1992) 441.
2. Hoof, O. V. Viviane, and M. E. D. Broe. *Crit Rev Clin Lab Sci.*, 31 (1994)197-293.
3. N. D'Onghia, and V. Casadio, *La Riforma Medica*, 66 (1952) 870.
4. M. M. Couttenye, P. C. D'Haese, V. O. V. Hoof, E. Lemoniatou, W. Goodman, et al. *Nephrology, dialysis, transplantation: official publication of the European Dialysis and Transplant Association - European Renal Association*, 11 (1996)1065-72.
5. C. S. Killian, F. P. Vargas, E. J. Pontes, S. Beckley, N. H. Slack, *Prostate*, 2 (1981) 187-206.
6. R. Olsson, C. Wesslau, T. Williamolsson, L. Zettergren, *Journal of Clinical Gastroenterolog*y, 11 (1989) 541-5.
7. J. Peng, X. X. Han Q. C. Zhang, H. Q. Yao, Z. N. Gao, *Analytica Chimica Acta*, 878(2015) 87-94.
8. L. F. Zhang, T. Hou, H. Y. Li and F. Li, *Analyst*, 140 (2015) 4030.
9. C. Fernandez-Sanchez and A. Costa-Garcia, *Electroanalysis*, 10(2015) 249-255.
10. C.C Shen, X. Z.Li, A. Rasooly, L. Y. Guo, K. N.Zhang, and M. H.Yang, *Biosensors & Bioelectronics*, 85(2016) 220.
11. H. Jiang and X. M. Wang, *Analytical Chemistry*, 84 (2012) 6986.
12. X. L. Ma, X. Zhang, X. L. Guo, Q. Kang, and D. Z. Shen, *Talanta*, 154(2016)175-182.
13. C. M. Li, S. J. Zhen, J. Wang, Y. F. Li, and C. Z. Huang, *Biosensors & Bioelectronics*, 43 (2013)366.
14. Q. Hu, B. Zhou, F. Li, J. Kong, and X. Zhang, *Chemistry, an Asian journal*, 11 (2016) 3040-3045.
15. J. Zhang, L. He, X. Zhang, and Z. P. Zhang, *Sensors & Actuators B Chemical*, 253(2017).
16. X. L. Hu, X. M. Wu, X. Fang, Z. J. Li, and G.L.Wang, *Biosensors & Bioelectronics*, 77(2015) 666.
17. X. G. Liu, X. J. Xing, B. Li, Y. M. Guo, Y. Z. Zhang, Y.Yang, and L. F. Zhang, *Biosensors & Bioelectronics*, 81(2016) 460-464.
18. L. Jia, J. P. Xu, D. Li, S. P. Pang, Y. Fang, Z. G. Song and J. Ji, *Chemical Communications*, 46 (2010)7166.
19. H. Huang, B. Wang, M. Chen, M. X. Liu, Y. Leng, X. Y. Liu, Y. X. Li, and Z. N. Liu, *Sensors & Actuators B Chemical*, 235(2016)356-361.
20. J. J. Deng, P. Yu, Y. X. Wang, and L.Q. Mao, *Analytical Chemistry*, 87(2015) 3080.
21. M. N. Zhang, K. Liu, K.P. Gong, L. Su, Y. Chen, and L.Q. Mao, *Analytical Chemistry*, 77 (2005) 6234-42.
22. M. Shan, M. Li, X. Y. Qiu, H. L. Qi, Q. Gao, and C.X. Zhang, *Gold Bulletin*, 47(2014) 57-64.
23. F. Y. Wang, Y.X. Li, W.Y. Li, Q. F. Zhang, J. Chen, H.P. Zhou, and C. Yu, *Analytical Methods*, 6 (2014)6105.
24. Y. Y. Zhang, Y. X. Li, C. Y. Zhang, Q. F. Zhang, X. A. Huang, M. Yang, S. A. Shahzad, K. W. Lo, C.Yu, and S. C. Jiang, *Analytical & Bioanalytical Chemistry*, 409 (2017)1.
25. H. Huang, B. Wang, M. Chen, M. X. Liu, Y. Leng, X.Y. Liu,Y. X. Li, and Z. N. Liu, *Sensors & Actuators B Chemical*, 235(2016)356.
26. H. T. Jiang, M. S. Islam, K. Sazawa, N. Hata, S. Taguchi, S. Nakamura, K. Sugawara and H. Kuramitz, *International Journal of Electrochemical Science*, 11 (2016) 5090 - 5102.

27. N. Tekaya, O. Saiapina, H. B. Ouada, F. Lagarde, H. B. Ouada, and N. Jaffrezic-Renault, *Bioelectrochemistry*, 90(2013)24-29.